# A kind of graphene film metamaterial for terahertz absorbers*

**GAO Run-mei** (高润梅)[1,2]**, **XU Zong-cheng** (续宗成)[1], **DING Chun-feng** (丁春峰)[1], and **YAO Jian-quan** (姚建铨)[1]

*1. Institute of Laser and Optoelectronics, College of Precision Instrument and Optoelectronics Engineering, Tianjin University, Tianjin 300072, China*

*2. College of Science, Guilin University of Technology, Guilin 541004, China*

(Received 9 October 2015)



A kind of functional graphene thin film metamaterial on a metal-plane separated by a thick dielectric layer is designed for terahertz (THz) absorbers. We investigate the properties of the graphene metamaterial with different interlayers in the 0–3 THz range. The simulation results show that the absorption rate reaches up to 99.9% at the frequency of 1.917 THz. Changing the period to 80 μm×18 μm can get a narrow-band high quality factor ($Q$) absorber. We present a novel theoretical interpretation based on the standing wave field theory, which shows that the coherent superposition of incident and reflection rays produces standing waves, and the field energy is localized inside the thick spacers and dissipates through the metal-planes.

**Document code:** A **Article ID:** 1673-1905(2016)01-0043-4

**DOI** 10.1007/s11801-016-5193-4

Recent researches have demonstrated that graphene is an efficient terahertz (THz) modulator[1-4]. The optical properties of graphene have attracted particular interest in the metamaterial and plasmonic polaritons[5-9]. More recently, graphene-based metamaterials with perfect absorption have been theoretically and experimentally studied, including the effective surface conductivity investigations of graphene micro-ribbon metamaterials and structured graphene metamaterials[10-14].

In this paper, we design a perfect absorber based on graphene, and demonstrate that the perfect absorption can be achieved by the patterned graphene microstructural arrays on a thick spacer deposited on a reflecting metal substrate. Numerical simulations and analytical calculations are used to investigate the perfect absorption and the surface current resulting from a local energy field in the absorber induced by CST 2009 and a standing wave effect.

We design a graphene metamaterial absorber with unit cell consisting of a graphene metamaterial and a thick dielectric interlayer deposited on the metal plane, as shown in Fig.1. One graphene micro-circle array and a metallic ground plane are separated by a thick dielectric spacer. The ground plane and the dielectric layer are copper metal and silicon (Si), respectively. The metagraphene has a radially periodic structure with period of 36 μm×36 μm, and the center of the circle is (0, 0). The Si dielectric with refractive index of $n=\sqrt{\varepsilon_d}=3.45$ is deposited on a copper metallic ground plane, and the thickness of Si dielectric spacer is $d$=33.4 μm. The copper metallic ground plate with conductivity of $\sigma=5.9\times10^7$ S/m and thickness of $t_2$=0.2 μm has perfect reflection property in the THz regime. The graphene is numerically modeled by a thin layer with thickness of $t_1$=0.5 nm and permittivity of $\varepsilon_{\text{eff}}=1+\sigma_s/\varepsilon_0\omega\Delta$ ($\Delta=t_1$), where $\sigma_s$ represents the conductivity of graphene, which can be derived using the well-known Kubo formula. The conductivity of graphene is described with interband and intraband parts as $\sigma_s=\sigma_s^{\text{intra}}+\sigma_s^{\text{inter}}$, where $\sigma_s^{\text{inter}}$ and $\sigma_s^{\text{intra}}$ are interband and intraband conductivities, respectively. At THz frequencies, the photon energy is $\hbar\omega<<E_F$, and the interband contribution is negligible compared with the intraband contribution. Therefore, the conductivity of graphene is well described by the Drude-like surface conductivity $\sigma_s\approx\sigma_s^{\text{intra}}$ for Fermi energy $E_F>>k_BT$ and $\omega\tau<<1$, and the conductivity of graphene depends linearly on the Fermi energy in the THz range as

$$\sigma_s \approx \frac{e^2 E_F \tau}{\pi\hbar^2}. \tag{1}$$

It can be seen from Eq.(1) that the conductivity is independent of frequency. We will design the graphene metamaterial for THz absorption by this approach.

* This work has been supported by the National Natural Science Foundation of China (Nos.61205096 and 11364010), and the Science Foundation of Education Department of Guangxi in China (No.200911LX17).

** E-mail: gaorm2002@aliyun.com

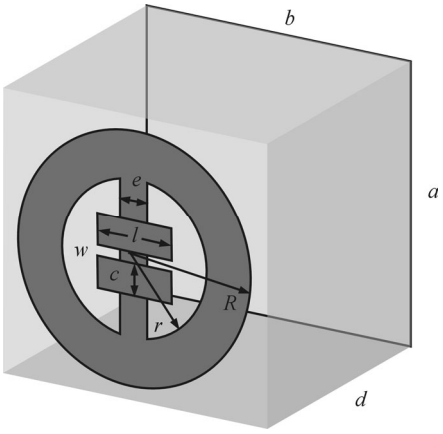


**Fig.1 Unit cell of the graphene metamaterial absorber structure, consisting of a graphene circular ring with *r*=10 μm, *R*=16 μm, *w*=1.5 μm, *c*=4 μm, *l*=10 μm, *e*=4 μm and thickness of $t_1$=0.5 nm, a silicon spacer with thickness of *d*=33.4 μm, and a copper ground plane with thickness of $t_2$=0.2 μm**

Numerical simulations are performed to investigate the absorption in the absorber by CST 2009. A THz wave normally incident on the interface between air and the circular ring of the metamaterial absorber is considered, and the numerically simulated absorption and reflection spectra for a 33.4 μm-thick Si spacer are shown in Fig.2. We can obtain a two-band perfect absorber. Varying the thickness of the spacer layer, the absorption spectra are shown in Fig.3. The band number of the absorber increases with the increase of spacer thickness. For example, a four-band absorber is obtained using a 56 μm-thick Si spacer in this THz frequency range. Changing the spacer material from Si to polyimide also can alter the absorption spectrum, as shown in Fig.4. The band number of the absorber and the peak frequencies are changed with the spacer material. Fig.5 shows the absorption spectra of the graphene metamaterial absorber using Si spacer with different thicknesses. It can be seen from Fig.5 that with the increase of Si spacer thickness, the absorption bandwidth becomes more and more narrow, and the number of absorption bands is increased. Fig.6 shows the comparison of absorption spectra of the graphene metamaterial absorbers using different dielectric materials as spacer layer with the same thickness of 23.1 μm. The relative permittivities of FR-4, alumina, polyimide, Si and gallium arsenide (GaAs) are 4.9, 9.4, 3.5, 11.9 and 12.9, respectively. With the increase of relative permittivity, the number of absorption bands is increased, the absorption bandwidth is more and more narrow, and the center frequency of absorption band is red shifted. The results indicate that the absorption spectrum in the unit cell structure is related with the geometric thickness and the material relative permittivity of the spacer layer.

To understand the absorption mechanism of the graphene metamaterial absorber, we investigate the surface current of one unit cell in the absorber with 56 μm-thick Si spacer layer. The distributions of the surface current at absorptive peak center frequencies of 0.363 THz, 1.143 THz, 1.917 THz and 2.679 THz and with absorption coefficients of 95.06%, 99.89%, 99.95% and 99.81% are shown in Fig.7(a)—(d), respectively. From Fig.7, we can note the conclusions as follows. First, the surface current exists on the top surface, the bottom surface and the metal ground. Second, the surface current distribution is periodic. There is one peak current at the first center frequency of 0.363 THz as shown in Fig.7(a), there are two peak currents at the second frequency of 1.143 THz as shown in Fig.7(b), and so on. Meanwhile, the spatial positions of peak currents are invariant for a fixed center frequency. Third, there is no current on the graphene structure surface, and the maximum current is found on the metal ground surface. The electromagnetic field presents a local distribution through the interaction between the metamaterial unit cell of the absorber and the incident field.

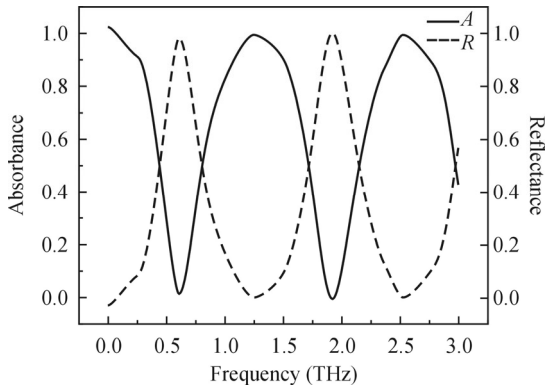


**Fig.2 Absorption and reflection spectra of the graphene metamaterial absorber with the Si dielectric spacer layer thickness of *d*=33.4 μm**

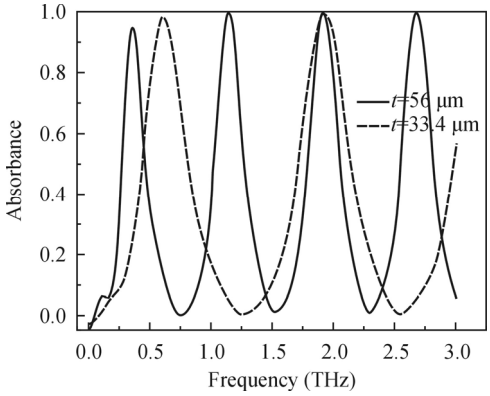


**Fig.3 Absorption spectra of the graphene metamaterial absorber using Si dielectric spacer layers with different thicknesses of 33.4 μm and 56 μm**

To provide a physical explanation, we consider the structure as an asymmetric Fabry-Perot cavity with two mirrors, i.e., a graphene micro-circle array as one mirror and the metal plate as the other one. The graphene micro-circle can be used as a metasurface due to its extremely small thickness compared with other dimensions and wavelength[15]. The absorption coefficient ($A$=1−$T$–$R$) is described using its reflection and transmission coefficients. The transmission of the system is completely suppressed by choosing a metal ground plate ($T$=0). To achieve total absorption of the incident energy ($A$≈1), the reflection must be equal to 0 as well

($R=|r|^2=|r_{12}+r_m|^2\approx0$, which is the sum of the direct reflection coefficient $r_{12}$ and the multiple reflection coefficient $r_m$).

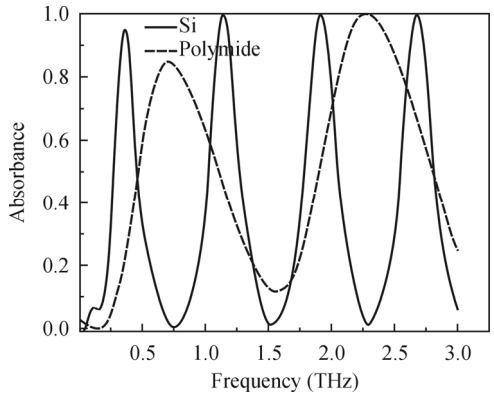


**Fig.4 Absorption spectra of the graphene metamaterial absorber using Si and polyimide dielectric spacer layers with the same thickness of 56 μm**

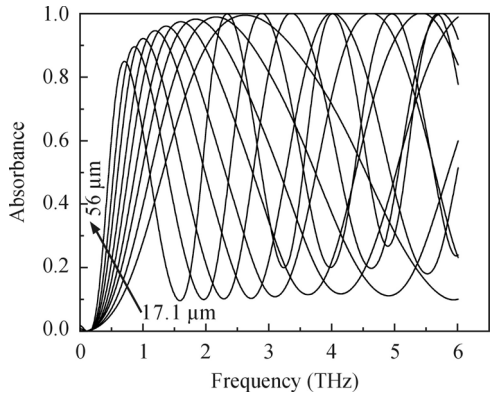


**Fig.5 Absorption spectra of the graphene metamaterial absorber using Si dielectric spacer layers with different thicknesses of 17.1 μm, 20.1 μm, 23.1 μm, 26.1 μm, 30.1 μm, 34.1 μm, 40.1 μm, 46.1 μm and 56 μm**

For the graphene metamaterial absorption, we use the standing wave theory to interpret it. The electromagnetic wave is normally incident on the air-graphene interface, and it is transmitted through the thick dielectric spacer interlayer and reflected at the metal ground. The reflected and incident waves form a standing wave. The normalized energy distribution in Fig.7(a) reveals that one peak is in the metal bottom surface and the adjacent node is in the air-graphene interface, in which the distance between them is a quarter of wavelength based on the standing wave theory. If we consider this distance as a segment, the number of segments is $N=4nlv/c$, the absorption peaks are located at $z=n'c/2nv$, and the distance between the maximum and minimum absorption is $\Delta x=c/4nv$, where $n$ and $l$ are the refractive index and thickness of the dielectric layer ($n=\sqrt{\varepsilon_p}$ and $l=d$), $c$ is the vacuum wave velocity, $n'$ is an integer, and $v$ is the incident wave frequency. $N$ is proportional to four times of the optical length $nl$, assuming frequency $v$ is a constant; otherwise it is linear with the frequency. The relationship between $N$ and the number of absorption bands $m$ satisfies $N=2m-1$. Compared with the theoretical values, the simulated number $N$ includes some error, which is likely due to our neglect of the differences in the refraction rate between the thin metal layer and the thick dielectric layer material. However, this does not affect the linear relationship between $N$ and the incident wave frequency $v$, as shown in Fig.8. The peak of the standing wave is located in the metal ground plate surface, while the node is located in the air-graphene surface because of the destructive interference resulting from the existence of half-wave loss at the air-graphene interface. The theoretical calculation agrees with the surface current distribution and the simulation results by finite integration method.

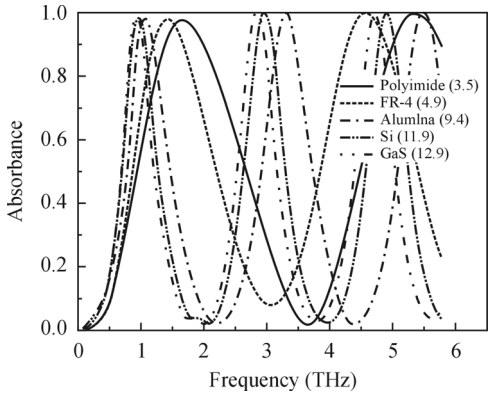


**Fig.6 Absorption spectra of the graphene metamaterial absorber using different dielectric spacer layers of polyimide, FR-4, alumina, Si and GaAs with the same thickness of 23.1 μm**

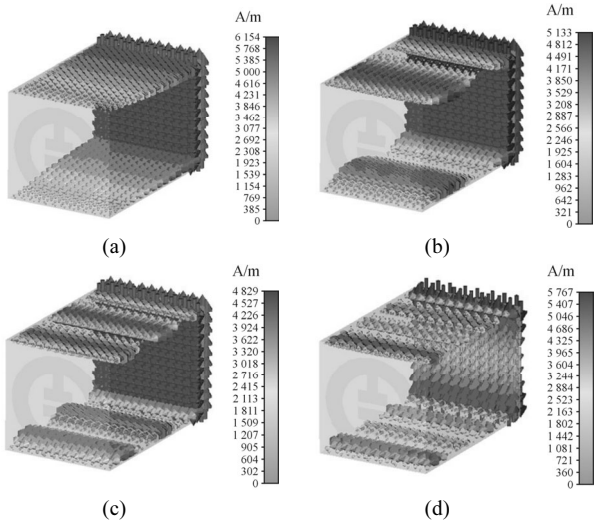


**Fig.7 Surface current distributions in one unit cell of the absorber with 56 μm-thick Si spacer layer at the center frequencies of (a) 0.363 THz, (b) 1.143 THz, (c) 1.917 THz and (d) 2.68 THz**

The electromagnetic field of the standing wave generates a local electric field, leading to the absorption of electromagnetic energy, which is the theoretical foundation of a perfect absorber. The absorptive peak frequency corresponds to the number of standing wave peaks. For example, at the third absorptive center frequency of 1.917 THz, there are three wave peaks in the standing

wave field in the dielectric spacer as shown in Fig.7(c). The absorptive center frequencies depend on 4*nl*. By controlling the optical length *nl*, a dielectric spacer can be designed with given frequency bands and center frequencies. These results reveal that fewer absorption bands and wider absorption bandwidths can be obtained by properly designing a dielectric spacer.

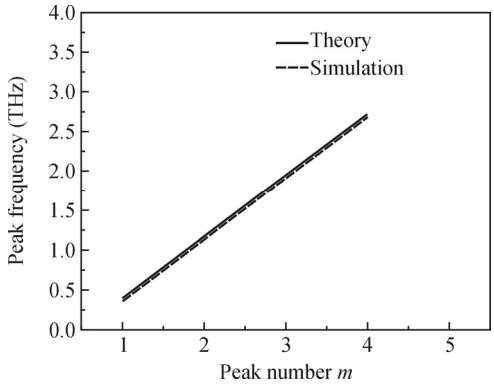


**Fig.8 The relationship between the number of the absorption bands and peak frequency**

A high quality factor (*Q*) narrow-band absorber can be obtained by using the structure period of 80 μm×18 μm, and each unit is constituted by three rings with the same size and structure. The medium layer is made of Si. When the thickness is 23.1 μm, there is only one absorption band with absorption peak frequency of *f*=1.504 THz, absorption coefficient of *A*=93.48%, absorption full width at half maximum (*FWHM*) bandwidth of 0.034 THz and *Q*=44. When the thickness is 33.4 μm, the absorption band is blue shifted, the absorption peak frequency is *f*=1.686 THz, and the absorption coefficient is raised to 99.79%, but the bandwidth changes to 0.092 THz which can be up to above 3 times, and the quality factor *Q* is decreased to 18.32. Absorption spectra of narrow-band high *Q* absorbers are shown in Fig.9. So the quality factor *Q* of the metamaterial absorber is related to the period of the metamaterial structure. We can obtain an absorber with high *Q* value and narrow band after geometry optimization.

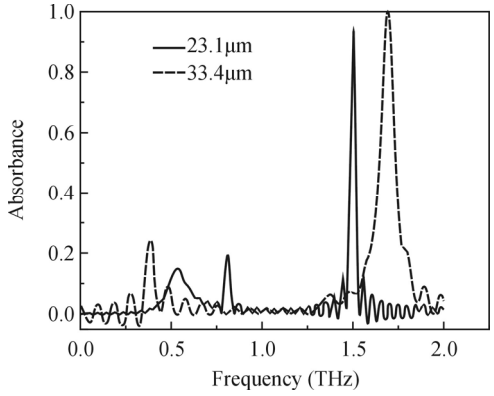


**Fig.9 Absorption spectra of the narrow-band high Q absorbers with period of 80 μm×18 μm using Si dielectric spacer layers with different thicknesses of 23.1 μm and 33.4 μm**

In summary, a graphene metamaterial perfect absorber is designed. The absorption band is linearly related to 4*nl* in the THz region. Four absorption bands are observed for the absorber with a 56 μm-thick Si spacer, and two absorption bands are observed for that with a 33.4 μm-thick Si spacer. The standing wave theory is used to explore the fundation of the absorber, and the predictions agree with the simulation results by CST. This theory shows that the incident and reflected waves in the metal ground undergo the coherent superposition to produce a standing wave, and the field energy is localized inside the spacer and dissipated completely. Based on the standing wave model, we investigate the surface currents through excitation and superposition, and it is found that the surface currents on the two sides of the spacer are clearly anti-parallel and the surface currents exhibit periodic variation in the ground plane. The research in this paper is valuable for the future development of metamaterial absorbers in the THz range.

## References

[1] M. D. He, G. Zhang, J. Q. Liu, J. B. Li, X. J. Wang, Z. R. Huang, L. L. Wang and X. S. Chen, Optics Express **22**, 6680 (2014).

[2] C. M. Watts, X. Liu and W. J. Padilla, Advanced Materials **24**, OP181 (2012).

[3] L. Ju, B. Geng, J. Horng, C. Girit, M. Martin, Z. Hao, H. A. Bechtel, X. Liang, A. Zettl, Y. R. Shen and F. Wang, Nature Nanotechnology **6**, 630 (2011).

[4] B. Sensale-Rodriguez, R. Yan, M. M. Kelly, T. Fang, K. Tahy, W. S. Hwang, D. Jena, L. Liu and H. G. Xing, Nature Communications **3**, 780 (2012).

[5] N. I. Landy, S. Sajuyigbe, J. J. Mock, D. R. Smith and W. J. Padilla, Physical Review Letters **100**, 207402 (2008).

[6] L. Huang, D. R. Chowdhury, S. Ramani, M. T. Reiten, S. N. Luo, A. K. Azad and H. T. Chen, Applied Physics Letters **101**, 101102 (2012).

[7] Y. S. Lin, C. Y. Huang and C. Lee, IEEE Journal of Selected Topics in Quantum Electronics **21**, 1 (2015).

[8] Y. J. Yoo, Y. J. Kim, J. S. Hwang, J. Y. Rhee, K. W. Kim, Y. H. Kim, H. Cheong, L. Y. Chen and Y. P. Lee, Applied Physics Letters **106**, 071105 (2015).

[9] G. Isić and R. Gajić, Journal of Applied Physics **116**, 233103 (2014).

[10] K. M. Wu, Y. J. Huang, T. L. Wanghuang, W. J. Chen and G. J. Wen, Applied Optics **54**, 299 (2015).

[11] X. G. Peralta, E. I. Smirnova, A. K. Azad, H. T. Chen, A. J. Taylor, I. Brener and J. F. O'Hara, Optics Express **17**, 773 (2009).

[12] L. Li, J. Wang, H. Du, J. Wang, S. Qu and Z. Xu, AIP Advances **5**, 017147 (2015).

[13] J. T. Hong, K. M. Lee, B. H. Son, S. J. Park, D. J. Park, Ji-Yong Park, Soonil Lee and Y. H. Ahn, Optics Express **21**, 7633 (2013).

[14] Z. W. Zheng, C. J. Zhao, S. B. Lu, Y. Chen, Y. Li, H. Zhang and S. C. Wen, Optics Express **20**, 23201 (2012).

[15] A. Tredicucci and M. S. Vitiello, IEEE Journal of Selected Topics in Quantum Electronics **11**, 130 (2014).